Design of a straw picking and cutting device

Kai Xu[1], Yanyan Ge[1,2*], Maohua Xiao[1], Min Kang[1], Jie Ni[1], Jinwu Wang[2]

(1. *College of Engineering, Nanjing Agricultural University, Nanjing 211800, China*;
2. *Shandong Daye Co., Ltd., Zhucheng 262218, Shandong, China*)

Abstract: In order to improve the effective recovery of straw, a new type of straw picking and cutting device was designed. A new type of roller moving knife mechanism was used which can realize simultaneous picking and cutting. A hammer claw was used to pick up and cut straw for the first time, and a roller moving knife was used to cut straw for the second time. ANSYS software was used to conduct static and modal analyses of the moving roller shaft and optimize the structure of the cutting part and the staggered arrangement of hammer claw. The first-order resonance frequency of the hammer claw shaft is 205.84 Hz, and the first-order natural frequency of the pulling roller moving knife mechanism is 214.35 Hz, which can avoid resonance and realize efficient picking and cutting of straw.

Keywords: straw, hammer claw, roller moving knife mechanism, fixed knife
DOI: 10.25165/j.ijabe.20211406.6746

Citation: Xu K, Ge Y Y, Xiao M H, Kang M, Ni J, Wang J W. Design of a straw picking and cutting device. Int J Agric & Biol Eng, 2021; 14(6): 93–98.

1 Introduction

Straw is a by-product of many crops, including wheat, corn, cotton, and sorghum. Straw is an indispensable raw material for the light industry, and it can effectively protect forest coverage. Straw can also be processed into "straw coal", which burns with minimal smoke and releases only 5% sulfur dioxide compared with those released by other types of coal[1]. With the massive consumption of energy and the promotion of a sustainable development strategy, straw recycling has nowadays become the main approach for straw disposal[2]. Using rapidly developing technology, the recycled straw is processed and can be used as biomass fuel, animal feed, organic fertilizer or for paper and fiberboard making[3-5], especially in the building industry, where straw has become one of the most favorite building materials for sustainable development[3,6]. This not only opens up a new way in old straw disposal, but, to a certain extent, alleviates resource scarcity and environmental pollution[2].

At present, some progress has been achieved in research on straw recovery devices in Europe and the USA. Agricultural machine manufacturers, such as Lely Industries N.V. (the Netherlands), CLAAS (Germany), and Strautmann (Germany), have relatively mature technology reserves. Although each product has its own advantages[7], their basic working principle is approximately the same. The common feature is the use of a pulling roller moving knife mechanism.

The development of straw picking and cutting devices in China is relatively backward. In 2017, Han et al.[8] developed a new saw disc straw crushing cutter, which had the advantages of strong cutting force and fast cutting speed. However, straw can get stuck easily. In 2019, a new cutting technology proposed by Zhao et al.[9] could cut straw on the ground by using a high-speed rotating chopper. However, the cutter shaft must rotate at a high speed and cut numerous times using a fixed knife, resulting in various problems, such as resonance.

Considering the existing problems in straw recycling devices, the current study designed a new straw picking and cutting device and further optimized its structure through reasonable analysis and simulation. This design uses a new cutting system with a pulling roller moving knife mechanism that works with a hammer claw, enabling the repeated cutting of straw. The secondary cutting method considerably improves cutting efficiency and prevents the phenomenon of stuck straw.

2 Overall structure and working principle

The straw picking and cutting device designed in the current study realizes efficient treatment of straw. The overall structure of the device is shown in Figure 1. A certain gap is maintained between the moving knife shaft (1) and the hammer claw shaft (2) to avoid interference. Simultaneously, the two axes should be at the same level to ensure that they will pick up straw in unison. The moving knives (3) are evenly distributed around the moving knife shaft (1) in two groups. The gap must be equal to ensure uniform force and deformation. The moving knives (3) cut the picked straw with the fixed knives at the back to complete the process. The hammer claw (4) adopts a staggered arrangement along the rotation axis (2) to ensure uniform force and smooth movement. The device can achieve synchronous pick up and cutting. The process is stable and prevents the stuck straw phenomenon.

3 Key component design and parameter determination

3.1 Design of the picking mechanism

3.1.1 Structure design of the hammer claw shaft

The material of the hammer claw shaft is 40CrNiMo steel. In accordance with the actual requirements of straw picking[10], the

Received date: 2021-02-14 **Accepted date:** 2021-10-24

Biographies: Kai Xu, Undergraduate, research interest: mechanical engineering, Email: xk214829@163.com; **Maohua Xiao,** PhD, Professor, research interest: mechanical engineering, Email: xiaomaohua@njau.edu.cn; **Min Kang,** PhD, Professor, research interest: Mechanical Engineering, Email: kangmin@njau.edu.cn; **Jie Ni,** Bachelor, research interest: mechanical engineering, Email: nijie@163.com; **Jinwu Wang**, Bachelor, Senior Engineer, research interest: materials science and engineering, Email: W62229981@126.com.

***Corresponding author: Yanyan Ge,** PhD, Associate Professor, research interest: development and application of Micro-nano biosensor and agricultural machinery equipment. College of Engineering, Nanjing Agricultural University, Nanjing 210031, China. Tel: +86-25-50606580, Email: yanyange@njau.edu.cn.

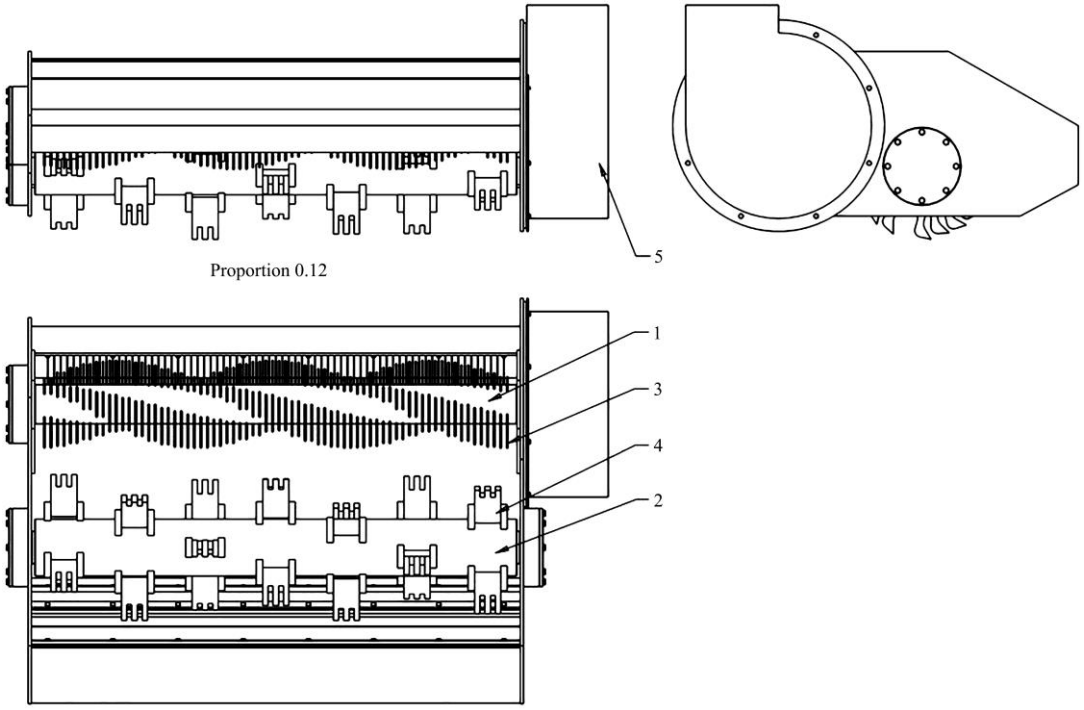

1. Moving knife shaft 2. Hammer claw shaft 3. Cutting knives 4. Hammer claw 5. Driving motor

Figure 1 Diagram of the overall structure

total length of the hammer claw shaft is set as 1.46 m and its diameter is set as 0.17 m to meet actual strength requirements. The final speed of the knife should be greater than 34 m/s[11] when straw is chopped. In accordance with relevant agricultural machine data, the speed of the driving shaft is determined as 2000 r/min and the maximum rotation radius of the hammer claw is $r = 0.28$ m. By calculating, a conclusion can be drawn that the speed of the hammer claw shaft is $v = 58.60$ m/s.

3.1.2 Structure design of the hammer claw

1) Selection of the bending angle and size of the hammer claw

We select the hammer claw with a bending angle of 147° in accordance with relevant information[12]. When the hammer claw collides with straw during high-speed rotation, the root will suffer from excessive stress. The force analysis of the hammer claw is illustrated in Figure 2.

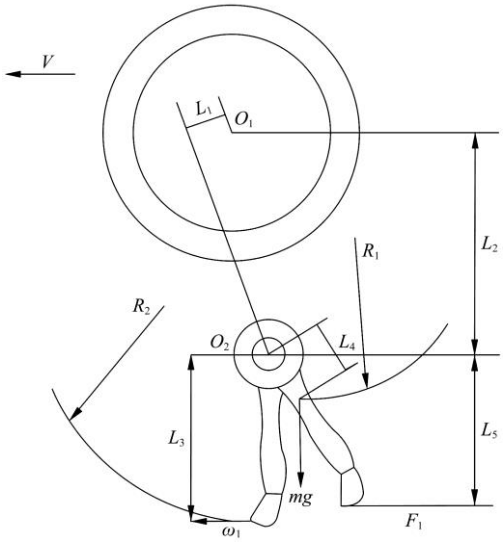

Figure 2 Force analysis diagram of the hammer claw

The following formula can be listed from the figure:

$$L_5 = L_3 \cos\theta \tag{1}$$

where, L_5 is the vertical distance between the center of the rotation axis and the point of action of resistance F_1, L_3 is the length of the hammer claw, and θ is the swing angle of the hammer claw.

$$F_2 = m\omega_1^2 R_1 \tag{2}$$

where, F_2 is the centripetal force of the hammer claw; m is the total mass of the hammer claw; ω_1 is the angular velocity of the hammer claw, and R_1 is the rotation radius of the hammer claw.

From the geometric relationship, the following expression can be obtained:

$$\frac{L_2}{R_1} = \frac{L_1}{L_4 \sin\theta} \tag{3}$$

where, L_1 is the distance between O_2 and O_1O_3 at the center of the rotation axis; L_2 is the distance between the center of rotation and the center of rotation axis, and L_4 is the straight-line distance between the center of mass of the hammer claw and the center of the hammer claw axis. The torque balance equation of the hammer claw relative to the center of the hammer claw shaft is

$$F_1 L_3 \cos\theta = mgL_4 \sin\theta + m\omega_1^2 L_2 L_4 \sin\theta \tag{4}$$

From Equation (4), the following equation is obtained:

$$\tan\theta = \frac{F_1}{m\dfrac{L_4}{L_3}(g + \omega_1^2 L_2)} \tag{5}$$

where, g is the acceleration due to gravity, which is 9.80 m/s^2.

When the hammer claw is working, the higher the value of θ, the greater the resistance of F_1, leading to a decrease in the straw picking rate[13]. Therefore, to fulfill actual work requirements, $R = 250$ mm. In accordance with the specific size requirements of the structure, the length of the hammer claw $L_3 = 130$ mm. On the basis of the preceding calculated size, the static calculation of the model is performed using the solution function to obtain the stress and deformation effect chart.

As shown in Figure 3, the maximum deformation is 0.0051 m, which meets actual requirements.

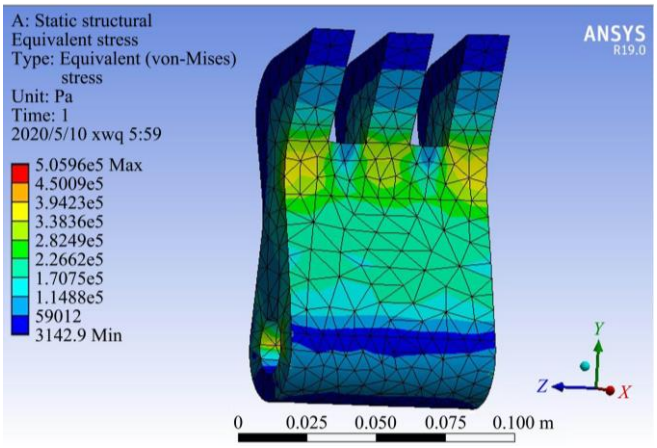

Figure 3 Diagram of hammer claw strain

2) Choice of hammer claw arrangement

The hammer claw arrangement of the picking device designed in this study is divided into spiral, staggered, and oblique symmetrical arrangements[11]. The most important factor of the device is smooth movement, for which, velocity and radial force are required to be small. The oblique symmetrical arrangement is mostly unstable, and thus, it is not considered. The spiral arrangement is nonuniform in terms of wear and should be replaced regularly. The designed device is required to operate in a harsh environment for a long period, worsening its wear and tear. Thus, we select the staggered arrangement.

3.2 Design of the cutting device

3.2.1 Composition and working principle of the cutting device

As shown in Figure 4, the cutting device is composed of a fixed cutting knife frame (1), fixed cutting knives (2), a roller shaft (3), cutting knives (4), and a motor (5). The fixed cutting knives (2) are evenly distributed on the fixed knife frame (1). A certain gap exists between adjacent fixed knives. The roller shaft (3) is connected to the motor shaft to obtain power. The cutting knives (4) are evenly distributed on the roller shaft (3) in a spiral arrangement. A pair of cutting knives has a certain gap between them[14].

Working principle: The motor (5) transfers power to the roller shaft (3). The roller shaft (3) drives the cutting knife (4) to rotate at a high speed. Straw is picked up between the two cutting knives. After half a rotation, cutting knife (4) cooperates with a fixed cutting knife (2) to cut straw into pieces. The cut straw is transferred to the next working stage through the weeding mechanism.

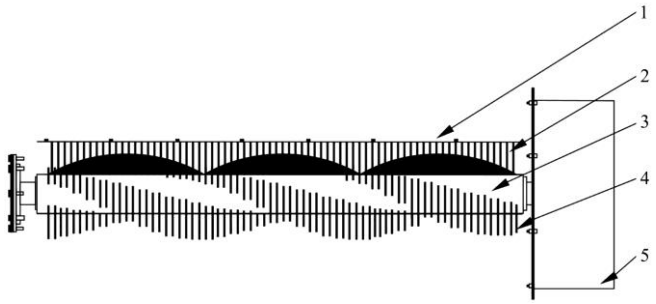

1. Fixed knife frame 2. Fixed cutting knife 3.Roller shaft 4. Cutting knife 5. Motor

Figure 4 Cutting mechanism

3.2.2 Design of the fixed cutting knife

The cutting edge of the fixed knife is a circular cutting edge. The blade material is 65Mn steel. Considering the life of the blade, its thickness is preliminarily determined as 5 mm, and the thickness of the cutting edge is 0.2 mm. Annealing treatment is performed. In addition, the distance between two fixed blades exerts a crucial effect on cutting efficiency; thus, the appropriate cutting clearance should be calculated[15].

The straw cutting process is a collaborative process between two cutting knives and a fixed knife. This cutting method is further transformed into a mechanical model. L_1 is the distance between the cutting knife and the fixed knife, L_2 is the thickness of the fixed blade, and L_3 is the gap between two fixed knives. Its 2D force model is depicted in Figure 5.

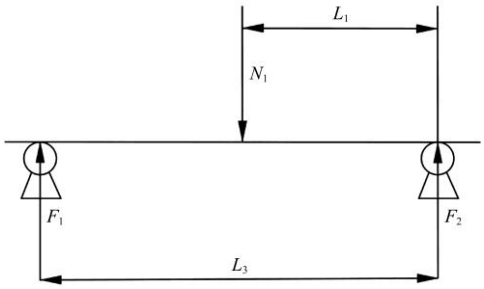

Figure 5 Diagram of the mechanical model

The N_1 received by the fixed knife is

$$N_1 = \frac{L_3 - L_1}{L_1} \cdot F_1 = \frac{L_3}{L_3 - L_1} \cdot F_2 \quad (6)$$

An external force F is added to the edge of the blade, and F = 180 N can be obtained from the calculation. In order to avoid fracture and other phenomena occur, the cutting edge of the knife is expanded, and the lower end is enlarged to 120 mm. Then, a simulation analysis is conducted.

As shown in Figure 6, the maximum stress at the end of the blade is 9833.70 Pa during this time. This value meets the specific practical requirements and is not easy to break.

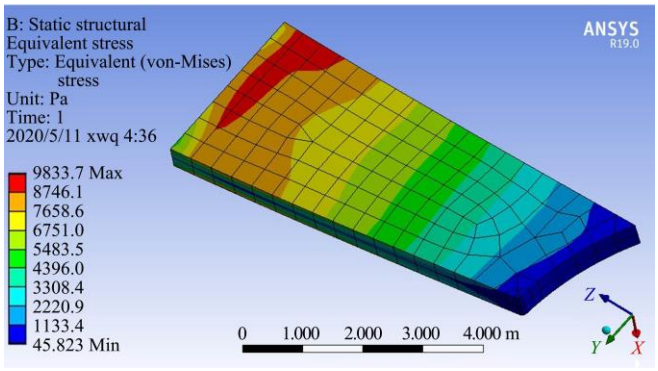

Figure 6 Diagram of fixed knife stress

2.2.3 Design of the cutting knife

The pulling roller moving knife mechanism adopts a double-row moving knife type; thus, two moving blades are distributed as a group of spirals on the roller shaft, and a certain clearance is controlled to make the moving blade and the fixed blade match[16]. The primary material of the blade is 65Mn, and Cr plating technology is used on the surface to ensure corrosion resistance. When the two moving blades are working, the size of the force exerted on them is different and affected by clearance. We must ensure that the stress of the heavy force side is within the allowable range.

As shown in Figure 7, the maximum cutting knife stress is found at the lower right corner, reaching a maximum of 7909.40 Pa. In accordance with the selected tool material parameters, the selected material can fully bear this stress level[17].

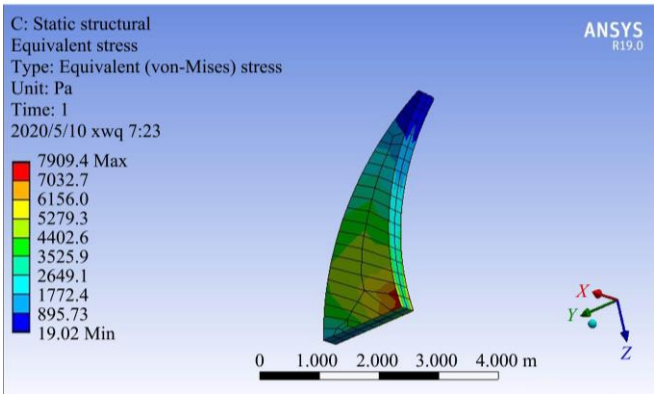

Figure 7 Diagram of cutting knife stress

3.2.4 Design of the roller shaft

The material 40MnB is selected to ensure the synchronicity of cutting and collecting. The shaft length is 1.50 m and the effective working length is 1.20 m, which are consistent with those of the collecting hammer claw shaft[18] in the picking mechanism.

In accordance with the material is 40MnB modulated steel, the allowable stress of the axis is 370 MPa. Thus, by calculation, we can determine that $d \geq 1.09$ m. We preliminarily assume that the diameter of the shaft is 1.10 m. Then, $d = 1.10$ m is substituted into the calculation to obtain the allowable deformation value of $\varphi = 0.00004718$ m < the shaft[19]. Thus, the diameter of the shaft is preliminarily determined to be qualified[20].

In accordance with the requirements of our actual field[15], to reasonably distribute the movable blades on the shaft, first of all, it is necessary to ensure that the tools are equally spaced in the axial direction and achieve equiangular distribution on the circumference. Therefore, the following settings are established: the number of knives is 16 because half of the cutting set should satisfy the number of moving knives, the moving blades should be 32 because the gap between the fixed knife and the cutting knife is 6 mm, and the clearance between the two moving knives of the knife group is 16 mm. On the basis of the aforementioned arrangement modes and parameters, the model is imported into ANSYS software for simulation analysis. The effect is illustrated in Figure 8.

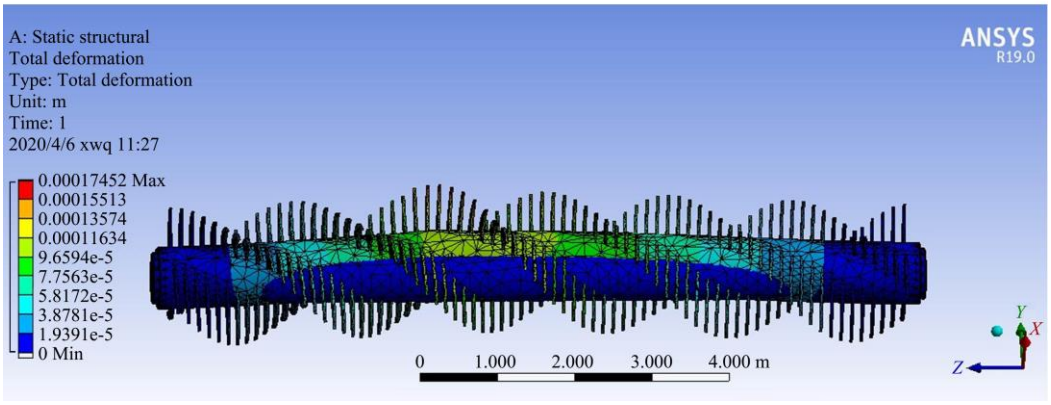

Figure 8 Strain diagram of the pulling roller moving knife mechanism

In accordance with the analysis figure, the maximum deformation of the roller shaft during operation is 0.0001 m, which meets the specific work requirements[21].

4 Modal analysis and simulation of high-speed motion axis

4.1 Modal analysis of the hammer claw shaft

Using the model function in the workbench to conduct modal analysis on the hammer claw shaft is crucial[10]. The 3D model is imported into ANSYS. Modal analysis of the model is performed, and the following results are obtained.

As indicated in Table 1, the first-order resonance frequency of the hammer claw shaft is 205.84 Hz and the rotational speed converted into the shaft is 12 351.88 r/min, which is considerably greater than rotational speed when it is operating; thus, the resonance problem can be completely avoided[22].

Table 1 Sixth-order natural frequencies and characteristics of the hammer claw shaft

Modal order number	Inherent frequency/Hz	Structural deformation
1	205.84	Severe bending of shaft center
2	206.16	Severe bending of shaft center
3	621.52	Severely bent shaft
4	623.00	Shaft breaks
5	652.80	Two sections of the shaft were fractured
6	767.09	Shaft breaks

4.2 Modal analysis of the roller pulling and moving knife mechanism

We import the 3D model into ANSYS, conduct modal analysis and simulation of the mechanism, and obtain the results.

As indicated in Table 2, the first-order natural frequency of the pulling roller moving knife mechanism is 214.35 Hz, which is converted into a shaft speed of 12 860.59 r/min. This value is faster than the speed of the roller shaft. Moreover, a rubber vibration damping pad is installed at the bottom of the mechanism support to prevent the resonance phenomenon completely[23].

Table 2 Sixth-order natural frequencies and characteristics of the hammer claw shaft

Modal order number	Inherent frequency/Hz	Structural deformation
1	214.35	Bending deformation of the shaft
2	214.60	Severe deformation of the shaft center
3	540.23	Shaft is severely bent
4	540.62	Bending deformation of the shaft
5	615.47	Shaft is completely deformed and broken
6	930.13	Shaft is broken

4.3 Adams dynamic simulation

After the structure optimization of the puller shaft, Adams software is used to conduct dynamic simulation to verify its workability. The results are presented in Figure 9.

As shown in Figure 9, resistance only changes slightly in the state of motion and will not cause a certain effect on the mechanism due to the considerable change in resistance.

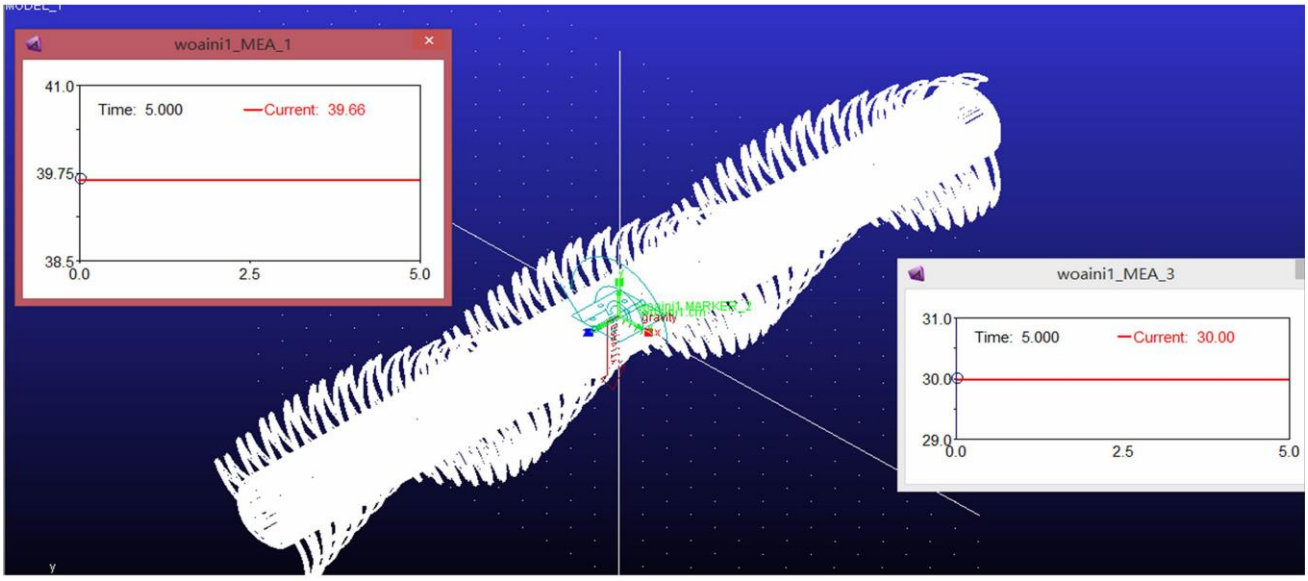

Figure 9 Diagram of Adams simulation analysis

5 Conclusions

1) To solve the problems of stuck straw and resonance in existing straw recycling devices, a new straw picking and cutting device was designed. This device can realize straw picking, recycling, and repeated cutting.

2) The key components of the structural design determine the relevant structure and location parameters. In accordance with the index requirements of the picking mechanism and the characteristics of the arrangement of the hammer and claw of various picking mechanisms, the staggered arrangement is adopted to reduce resistance and increase working speed. The structure and size of the hammer claw are determined via a detailed calculation and static analysis.

3) Modal analysis and simulation are performed on a high-speed moving shaft to avoid resonance, ensuring that the entire device can achieve its best performance in a harsh field environment.

Acknowledgements

This work was financially supported by Jiangsu Agricultural Science and Technology Innovation Fund of China (CX (19)3071), the Fundamental Research Funds for the Central Universities (KYXK2021001) and the High-Level Talent Project of "Six Talent Peaks" in Jiangsu Province of China (GDZB-023).

Nomenclature

ω	angular velocity of the driving shaft (rad/s)
v	rotational speed of the hammer claw shaft (m/s)
r	slewing radius of the hammer claw (m)
θ	swing angle of the hammer claw (°)
L	length (m)
m	mass (kg)
R	rotation radius of the hammer claw (m)
F	force (N)
g	acceleration of gravity (m/s^2)
N	force on the blade (N)
d	diameter of the roller shaft (m)
φ	deformation allowable value of the shaft

[References]

[1] Li H, Shen W Q, Ban T. Research progress of the use of technology and crushing equipment on straw in China. Journal of Chinese Agricultural Mechanization, 2018; 1: 17–21. (in Chinese)

[2] Wang Q Q, Jiang Y C, Li L H, Qin J W, Chen L Q. Performance analysis of a spring-tooth drum pickup of straw baler via coupling simulation. Int J Agric & Biol Eng, 2021; 14(4): 159–165.

[3] Cornaro C, Zanella V, Robazza P, Belloni E, Buratti C. An innovative straw bale wall package for sustainable buildings: experimental characterization, energy and environmental performance assessment. Energy & Buildings, 2020; 208: 109636. doi: 10.1016/j.enbuild.2019.109636.

[4] Chen L, Wang H, Huang Y Z, Ping Z W, Yu M, Zheng X F, et al. Robust hierarchical sliding mode control of a two-wheeled self-balancing vehicle using perturbation estimation. Mechanical Systems and Signal Processing, 2020; 139: 106584. doi: 10.1016/j.ymssp.2019.106584.

[5] Espinosa E, Rol F, Bras J, Rodriguez A. Production of lignocellulose nanoflbers from wheat straw by different fibrillation methods. Comparison of its viability in cardboard recycling process. Journal of Cleaner Production, 2019; 239: 118083. doi: 10.1016/j.jclepro.2019.118083.

[6] Koh C, Kraniotis D. A review of material properties and performance of straw bale as building material. Construction and Building Materials, 2020; 259: 120385. doi: 10.1016/j.conbuildmat.2020.120385.

[7] Du J N, Han B S, Tian H Q, Wang P F, Jiang H D, Guo K. Analysis and study of the main factors affecting the performance of hammer mill. Journal of Agricultural Mechanization Research, 2015; 3: 54–57.

[8] Han X M, Zhang J, Gao Y C, Zhang J W, Yu Y T, Geng A J. Design and test of saw disc straw crushing returning machine. Journal of Chinese Agricultural Mechanization, 2017; 38(12): 7–11. (in Chinese)

[9] Zhao X J, Wang J Y, Dai X J, Yang L, Gao X H. Design and simulation analysis of straw cutting and crumbing device. Agricultural Engineering, 2019; 4: 023. doi: 10.3969/j.issn.2095-1795.2019.04.023.

[10] Tang Z, Zhang B, Liu X, Ren H, Li X Y, Li Y M. Structural model and bundling capacity of crawler picking and baling machine for straw wasted in field. Computers and Electronics in Agriculture, 2020; 175(1): 105622. doi: 10.1016/j.compag.2020.105622.

[11] Qiu J, Wu M L, Guan C Y, Fang Y X, Li X C. Design and experiment of chopping device with dynamic fixed knife coaxial for rice straw. Transactions of the CSAE, 2015; 31(10): 11–19. (in Chinese)

[12] Chang H Q, Zhu X H, Wu J, Guo D Y, Zhang L H, Feng Y. Dynamics of microbial diversity during the composting of agricultural straw. Journal of Integrative Agriculture, 2021; 20(5): 1121–1136.

[13] Zhang J, Yu Y T, Yang Q Y, Zhang J W, Zhang Z L, Geng A J. Design and experiment of smashed straw unit for high stubble maize double header. Transactions of the CSAM, 2018; 49(S1): 42–49. (in Chinese)

[14] Marinov V R. Hybrid analytical–numerical solution for the shear angle in orthogonal metal cutting — Part I: theoretical foundation. International

Journal of Mechanical Sciences, 2001; 43(2): 399–414.
[15] Yin Y X, Qin W C, Zhang Y W, Chen L P, Wen J Q, Zhao C J, et al. Compensation control strategy for the cutting frequency of the cutterbar of a combine harvester. Biosystems Engineering, 2021; 204: 235–246.
[16] Brockman J S. Book review: Straw for fuel, feed and fertiliser? Outlook on Agriculture, 1983; 12(2): 100. doi: 10.1177/ 003072708301200219.
[17] Han G P, Umemura K, Kawai S, Kajita H. Improvement mechanism of bondability in UF-bonded reed and wheat straw boards by silane coupling agent and extraction treatments. Journal of Wood Science, 1999; 45(4): 299–305.
[18] Belhadj B, Bederina M, Montrelay N, Houessou J, Quéneudec M. Effect of substitution of wood shavings by barley straws on the physico-mechanical properties of lightweight sand concrete. Construction & Building Materials, 2014; 66: 247–258.
[19] Zhang J X, Wang X N, Chen F, Jiang Y X, Niu C H. Study on working parameters of knife roller of field straw chopper for mulching or reclaiming. Transactions of the CSAM, 2007; 38(6): 82–85.(in Chinese)
[20] Goodhew S, Griffiths R, Woolley T. An investigation of the moisture content in the walls of a straw-bale building. Building and Environment, 2004; 39(12): 1443–1451.
[21] Demirba A, Ahin A. Evaluation of biomass residue : 1. Briquetting waste paper and wheat straw mixtures. Fuel Processing Technology, 1998; 55(2): 175–183.
[22] Hironori, Arai, Yasukazu, Hosen, Van, Nguyen, et al. Greenhouse gas emissions from rice straw burning and straw-mushroom cultivation in a triple rice cropping system in the Mekong Delta. Soil Science and Plant Nutrition, 2015; 61(4): 719–735.
[23] Lantz M, Svensson M, Bjoernsson L, Boerjesson P. The prospects for an expansion of biogas systems in Sweden—Incentives, barriers and potentials. Energy Policy, 2007; 35(3): 1830–1843